# Influence of carbon aerogel texture on PEMFC performances

Mathilde Brigaudet, Sandrine Berthon-Fabry, Christian Beauger, Marian Chatenet, Patrick Achard

# INFLUENCE OF CARBON AEROGEL TEXTURE ON PEMFC PERFORMANCES

**M. BRIGAUDET[1,*], S. BERTHON-FABRY[1], C. BEAUGER[1], M. CHATENET[2], P. ACHARD[1]**

[1]Mines ParisTech, CEP - Centre Energétique et Procédés, CNRS FRE 2861
BP 207, 1 rue Claude Daunesse, 06904 Sophia Antipolis, France

[2]Laboratoire d'Electrochimie et de Physicochimie des Matériaux et des Interfaces (LEPMI),
UMR 5631 CNRS-INPG-UJF, BP 75, 38402 Saint Martin d'Hères Cedex, France

(*author for correspondence, e-mail: mathilde.brigaudet@mines-paristech.fr)

## ABSTRACT

To improve Proton Exchange Membrane Fuel Cells (PEMFC), it is necessary to understand the phenomena occurring in operating conditions. The objective of this study is to determine how carbon support architecture can impact PEMFC performances, particularly diffusive limitations. In this context, as they have a controllable texture, carbon aerogels were used as catalyst supports in PEM fuel cell cathodes. Three carbon aerogels with different morphologies were synthesized. Fuel cell measurements show that the carbon support architecture has a significant impact on diffusive limitations. Moreover, they confirm that Nafion® loading must be optimized in order to preserve the catalytic layers architecture. This work finally highlights the impact of the catalytic layers architecture on the PEMFC performances.

## 1. INTRODUCTION

Proton Exchange Membrane Fuel Cells (PEMFC) have been studied for many years. These researches have cost reduction as a main objective, in order to make PEMFC competitive. Reducing the costs mostly implies both diminishing the platinum quantity required for the oxygen reduction reaction at the cathode and increasing its activity. For these reasons, researches are devoted to the development of new electrocatalysts and to the understanding of the phenomena occurring in fuel cells.

Nowadays, state-of-the-art PEMFC electrodes supports are made of carbon blacks. However, these carbons (and as a consequence the catalytic layers) do not have a controlled texture. As a result, it is hard to understand the diffusive phenomena limiting the electrochemical performances. By contrast, carbon aerogels present a controllable texture [1,2,3] and are thus suitable PEMFC electrodes catalysts supports: they conduct electrons and are permeable to reactant gases. Carbon aerogels have already been used in PEMFC electrodes [4,5] but the particle size and the pore size distribution effects on gas diffusion have never been optimised [6]. In addition, the impact of Nafion® loading with this kind of materials was only evaluated towards the oxygen reduction reaction studied in dedicated 3-electrode cell in the presence of liquid electrolyte, but not in a Membrane Electrode Assembly (MEA) [7]. The objective of this study is thus to identify the main parameters influencing diffusive limitations in a MEA. For that purpose, the impact of Nafion® loading was measured for a single carbon aerogel morphology. In addition, three very different carbon aerogels morphologies were synthesized and "doped" with platinum to confirm the role of the Pt catalyst support on the ORR kinetics and utilization factor of the Pt.

## 2. EXPERIMENTAL

### 2.1 Carbon aerogel synthesis

Three carbon aerogels were prepared following Pekala's method [8]. Gels are obtained by polycondensation of resorcinol (R) with formaldehyde (F) (with a molar ratio F/R=2) and water in the presence of $Na_2CO_3$ (C). To obtain three different morphologies (see Table 1) we have varied the reagents molar ratio (R/C) and the mass fraction of reagents in the sol (%solid defined as $(m_R+m_F+m_C)/m_{H2O}*100$). R/C and %solid respectively affect the particles size and aerogels density. After gelation, the gels were placed in successive acetone baths during one week for exchanging water filling the pores of the gels. The

gels were then dried under $CO_2$ supercritical conditions [9, 10]. Afterwards, the dry organic aerogels were pyrolyzed at 1050°C during 30 minutes under a nitrogen flow (5 L/min), thus yielding carbon aerogels.

**2.2 Catalyst preparation**

Carbon aerogels are first ground to obtain fine powder. Powder samples are then suspended in a $H_2PtCl_6$ water solution with a platinum concentration of 0.6 g/L and a mass ratio Pt/(Pt+C) equal to 35 wt% (final targeted mass ratio Pt/(Pt+C) is 30 wt%). After 24 h of magnetic stirring, the reducing agent $NaBH_4$ is added in the suspension as an aqueous solution (0.6 M). $NaBH_4$ is added in large excess during 24 h under magnetic stirring thus ensuring complete platinum salt reduction. Pt-doped carbon aerogel powder is then washed several times with boiling water, filtered and dried at 100°C for one night. The dry powder obtained is placed in a tubular quartz furnace to undergo thermal treatment. Should platinum salt remain on the carbon surface upon this treatment, we first decomposed it at 350°C under nitrogen flow for 30 minutes and then achieved its reduction by changing nitrogen to hydrogen for 30 minutes. The system cooling occurs under a nitrogen flow.

However, despite this procedure, the Pt/C catalysts obtained did not present exactly the expected Pt/(Pt+C) mass ratio (see Table 1 and Table 2). The procedure was repeated and presented reproducible results. So the low platinum loading of C must be due to carbon geometry that is not adapted.

**2.3 Catalyst and carbon aerogel characterization**

Carbon aerogels were characterized by $N_2$ sorption and Hg porosimetry. $N_2$ sorption enables measuring the BET surface area ($S_{BET}$) and characterizing the microporous (pores smaller than 2 nm) and mesoporous volume (pores smaller than 50 nm) while Hg porosimetry characterizes the volume of pores larger than 7.5 nm, thus giving information on the macroporous volume.

Transmission Electron Microscopy (TEM) allowed us to evaluate the distribution and the size of the platinum particles in the catalysts.

**2.4 MEA preparation**

Membrane-Electrode Assemblies (MEA) are realized with the decal method [11]. The cathode catalyst ink is prepared by magnetically stirring Pt-doped carbon aerogel powder, 0.3 wt%-Nafion® solution (dilution with deionized water of DE 1020, Ion Power Inc) and deionized water. In the study of the influence of the carbon aerogel architecture, all the MEA have a constant Nafion®/carbon mass ratio (N/C) equal to 1. On one of the studied architectures, the Nafion® loading was varied to evaluate its impact on the MEA performances. The corresponding amount of catalyst ink is then sprayed on a Kapton® sheet in order to obtain a cathodic Pt loading in the MEA of 0.5 mg/cm² (the cathode has a 50 cm² active geometric surface area). The Kapton® sheet is then hot pressed on a Nafion® N112 membrane with a commercial anode from PAXITECH. MEA are finally obtained by hot-pressing, a commercial GDL and cell gaskets, in a second step.

**2.5. Fuel cell tests**

Experiments are conducted on a homemade monocell test bench [11]. The fuel cells performances are evaluated at operating cell temperature of 73°C and pressure of 1.3 bar. Hydrogen and air are used as reactant gases with a respective stoichiometry of 2 and 2.5. The relative humidity is kept at 100 % for both gases. A minimum flow rate is applied for the inlet gases when cell intensity is lower than 12 A: 30 nL/h for air and 10 nL/h for hydrogen. The cell is electrically controlled using a potentiostat (Bio-Logic, HCP-803).

Each new MEA is submitted to a start-up procedure, improving slowly the performance until stabilization. Experimental Ui plots are determined by fixing the voltage (for increasing and decreasing voltages) and measuring the intensity. For each fixed voltage, the intensity is determined as the average of the two experimental values obtained while increasing or decreasing the voltage and after 5 min stabilization.

Impedance spectroscopy and cyclic voltammetry are used to determine the MEA ohmic resistance and the active surface area of platinum. $H_2$ crossover current density has also been measured applying a voltage of 0.5V at the $N_2$ fed electrode and measuring the oxidation current, the other electrode still being fed with $H_2$.

## 3. RESULTS & DISCUSSION

### 3.1 Carbon aerogels texture and catalysts characteristics

Carbon aerogels characteristics and Pt loadings are reported in Table 1.

Table 1. Carbon aerogels and catalysts characteristics

| Sample | %solid | R/C | Pt/ (Pt+C) | $S_{BET}$ ($m^2/g$) ± 5 | $V_{(0-2\ nm)}$ ($cm^3/g$) ± 0.01 | $V_{(2-7.5\ nm)}$ ($cm^3/g$) | $V_{Hg}$ ($cm^3/g$) ± 0.05 | $V_V$ ($cm^3/g$) ± 0.1 | Mean mesopore diameter (nm) ± 2 |
|---|---|---|---|---|---|---|---|---|---|
| A | 5 | 200 | 31 | 649 | 0.29 | 0.11 | NA | NA | 26 |
| B | 10 | 200 | 31 | 546 | 0.24 | 0.10 | 4.39 | 4.7 | 27 |
| C | 10 | 50 | 22 | 445 | 0.19 | NA | 0.65 | 0.8 | 8 |

$V_{(0-2\ nm)}$ refers to the microporous volume calculated from Dubinin-Radushkevich equation. $V_{(2-7.5\ nm)}$ refers to the mesoporous volume of pores comprised between 2 and 7.5 nm and is evaluated thanks to $N_2$ sorption. $V_{Hg}$ corresponds to the volume of mercury introduced during Hg porosimetry. $V_v$ is the total pore volume and is calculated as follows: $V_v = V_{(0-2\ nm)} + V_{(2-7.5\ nm)} + V_{Hg}$.

The synthesis led to samples with an increasing density. A and B present a pore size distribution with different scales (microporous, mesoporous and macroporous) with a lower BET surface area for B. C is mesoporous with few micropores leading to a lower total pore volume than B.

The TEM micrographs (Figure 1) of the three catalysts show that platinum is quite well spread on the different carbon aerogels whatever $S_{BET}$. However, platinum aggregates can be distinguished particularly on B/31 and C/22, which is probably related to the reduction process with $NaBH_4$. Catalysts are labeled as follows: Carbon aerogel/(Pt/(Pt+C)).

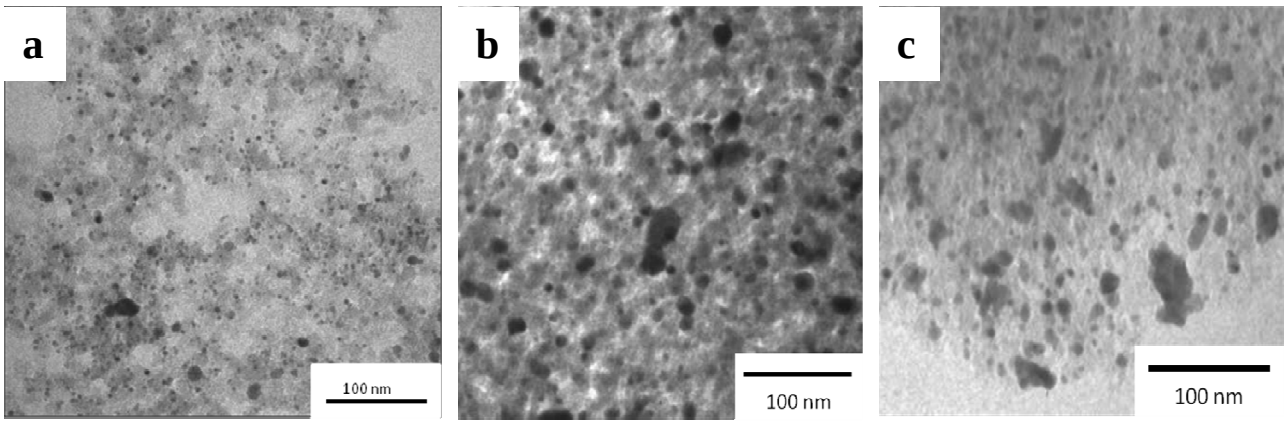


Figure 1. TEM micrographs of catalysts A/31 (a), B/31 (b) and C/22 (c)

### 3.2 Nafion loading impact on cell performances

To complete a recent study [7], we chose the carbon aerogel morphology B to evaluate the influence of Nafion® loading. Nafion®/Carbon mass ratio (N/C) was chosen as 0.5, 1 and 2. One drawback of the decal method is a loss of catalytic ink by removing the Kapton® sheet. Consequently, the MEA did not all have the expected cathodic Pt loading (0.5 mg/cm²).

The characteristics of our MEA are reported in Table 2. $S_{Pt}$ refers to the active platinum surface area at the cathode and r is the resistance of the MEA. The discrepancy between the different resistance values is probably due to the different thicknesses of the catalytic layers and to the insulating properties of Nafion®.

Table 2. MEA characterization

| Sample | %solid | R/C | Pt/ (Pt+C) | Pt loading (mg/cm²) | N/C | $S_{Pt}$ ($m^2/g_{Pt}$) | r (mΩ) | $i_{crossover}$ (mA) | Tafel slope (mV/dec) |
|---|---|---|---|---|---|---|---|---|---|
| B1 | 10 | 200 | 31 | 0.19 | 0.5 | 18.5 | 3.7 | 131 | -114 |
| B2 | 10 | 200 | 31 | 0.49 | 1 | 12.3 | 6.2 | 85 | -96 |
| B3 | 10 | 200 | 26 | 0.45 | 2 | 4.2 | 7.0 | 129 | -176 |

The polarization curves are presented in Figure 2. The best performances are obtained with N/C=1 (mass ratio). The performances are quite similar with N/C equal to 0.5 but slightly decrease at high current density. For N/C=2, the cell voltage decreases quicker when the current density increases.

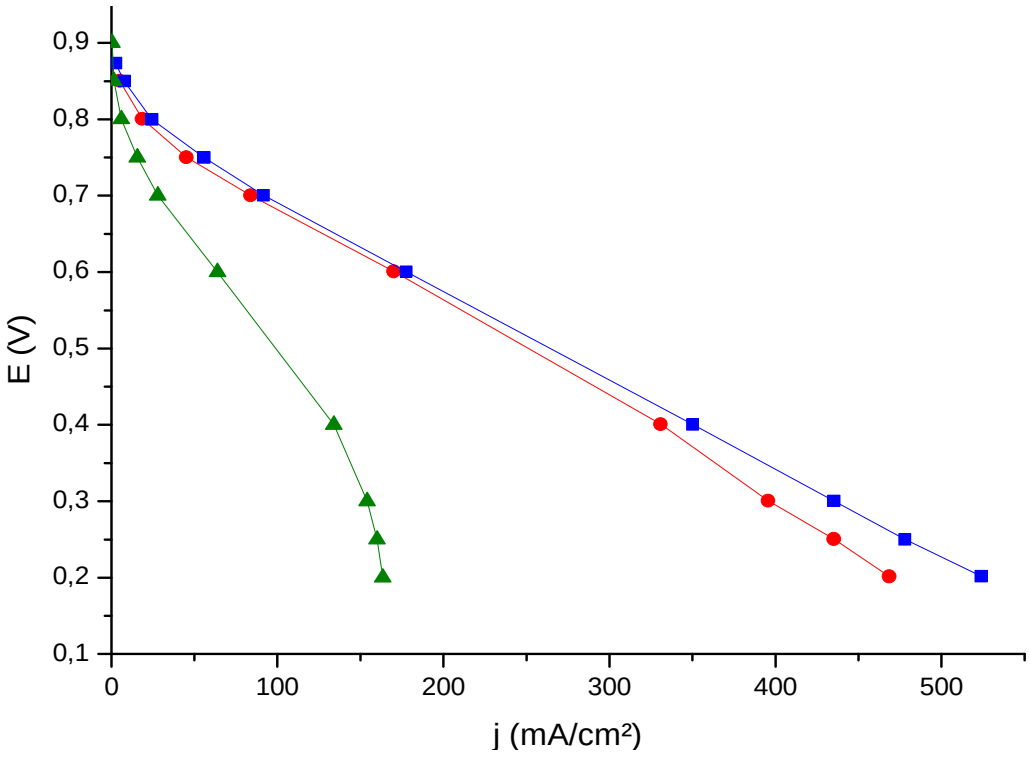


Figure 2. Cell voltage vs. experimental current density for B1 (N/C=0.5) (●), B2 (N/C=1) (■) and B3 (N/C=2) (▲).

The MEA performances are analyzed by separating the different contributions to losses. It is well known that the thermodynamic reversible cell potential is diminished by (i) activation losses ($\eta_{ORR}$) due to limited $O_2$ reduction kinetics, (ii) ohmic losses ($\eta_{Ohm}$) due to membrane and catalytic layers resistance along with contact quality between the different elements of the cell, (iii) diffusive losses ($\eta_{diff}$) due to limited gases and water diffusion in the electrodes.

In such systems, activation and diffusion losses in the anode are neglected [6, 12]. Gasteiger et al. [12] have elaborated a methodology to evaluate these different contributions.

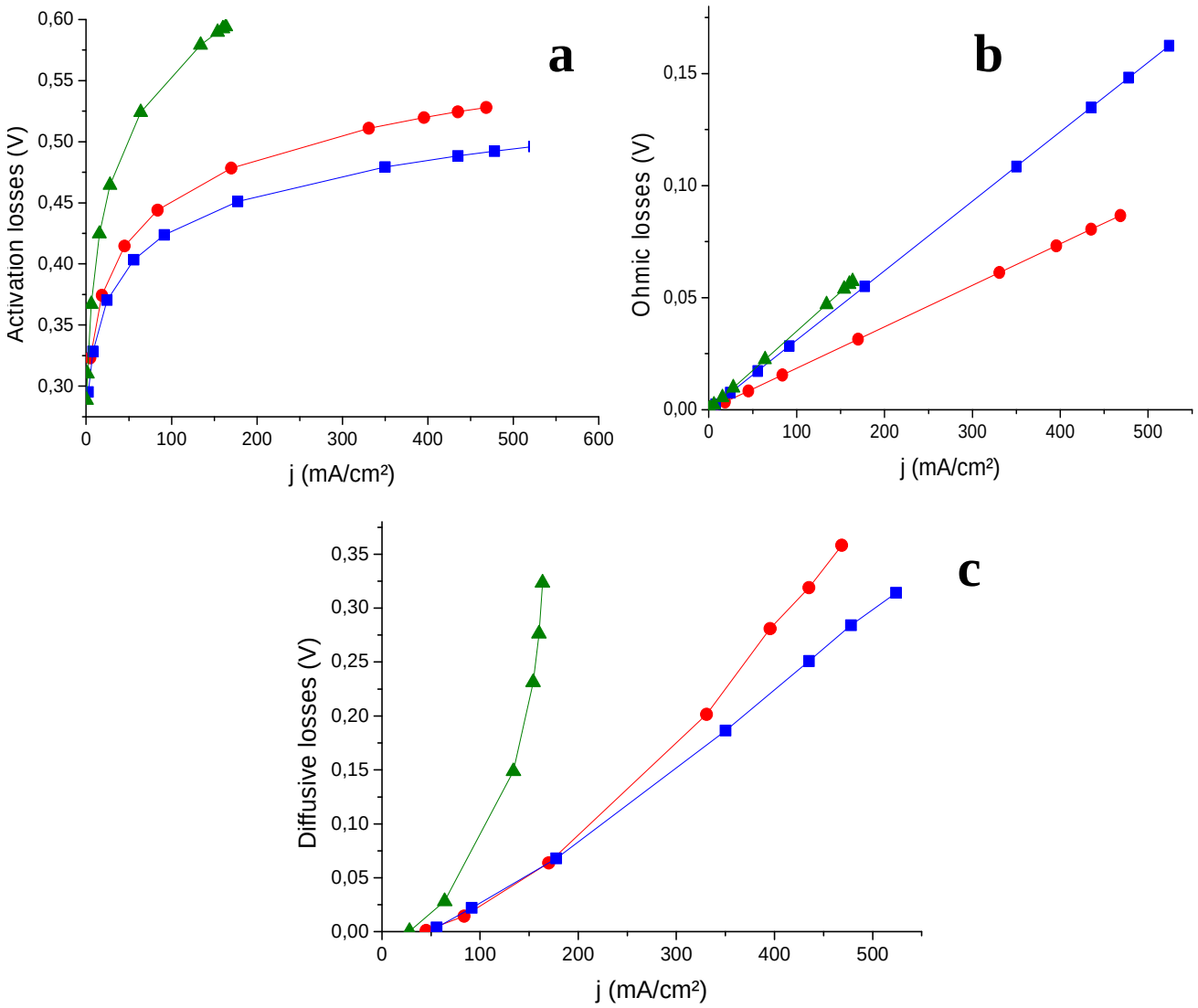


Figure 3. Activation losses (a), ohmic losses (b) and diffusive losses (c) of B1 (N/C=0.5) (●), B2 (N/C=1) (■) and B3 (N/C=2) (▲).

Figure 3 represents the different contributions to losses for MEA with different Nafion® loadings. The lowest activation losses (Figure 3a) are obtained with N/C=1 (B2). When N/C=0.5 (B1), activation losses are more important in spite of a higher active platinum surface area (Table 2). This is due to a lack of Nafion®, which leads to a poor ionic conductivity as explained by Passalacqua et al. [13]. When Nafion® is in excess (N/C=2, B3), platinum particles are insulated, which is confirmed by a low active platinum surface area (Table 2).

As explained above, different thicknesses of catalytic layers explain such ohmic losses (Figure 3b). Regarding diffusive losses (Figure 3c), an excess of Nafion® greatly affects gas diffusion. Guilminot et al. [14] demonstrated that Nafion® (in aqueous solution) increases diffusive losses. Indeed, when there is too much Nafion®, the Nafion® layer is certainly thicker (it can ultimately completely fill the pores of the active layer), which probably hinders $O_2$ diffusion to the reaction sites and diminishes the overall ORR kinetics. This is particularly the case for B3.

Although interesting, these results must however be confirmed since B1 has a lower Pt loading than B2 and B3. Therefore, we cannot rule out that the differences of performances we monitored origin from different Pt loading and not to different Nafion® loading.

### 3.3 Influence of carbon aerogel architecture on cell performances

As previously explained, it is difficult to obtain the expected cathodic Pt loading (0.5 mg/cm²). The characteristics of the MEA are presented in Table 3. Considering the first parameters ($S_{Pt}$ and r), the performances of A* and C* appear quite similar. However, there is a discrepancy between the Tafel slope values. B* exhibits a higher resistance and a lower active platinum surface area.

Table 3. MEA characterization

| Sample | %solid | R/C | Pt/ (Pt+C) | Pt loading (mg/cm²) | N/C | $S_{Pt}$ ($m^2/g_{Pt}$) | r (mΩ) | $i_{crossover}$ (mA) | Tafel slope (mV/dec) |
|---|---|---|---|---|---|---|---|---|---|
| A* | 5 | 200 | 31 | 0.49 | 1 | 25.4 | 4.1 | 102 | -101 |
| B* | 10 | 200 | 31 | 0.49 | 1 | 12.3 | 6.2 | 85 | -96 |
| C* | 10 | 50 | 22 | 0.43 | 1 | 25.5 | 4.3 | 168 | -192 |

* Texture of A, B and C used for catalytic layer

The polarization curves, presented in Figure 4, reveal that the best performances are obtained with aerogel A*. It must be reminded that all MEAs have been made and tested in exactly the same conditions. So the differences observed are likely not due to the slightly different Pt loadings but most probably to the type of aerogels used or better interfaces.

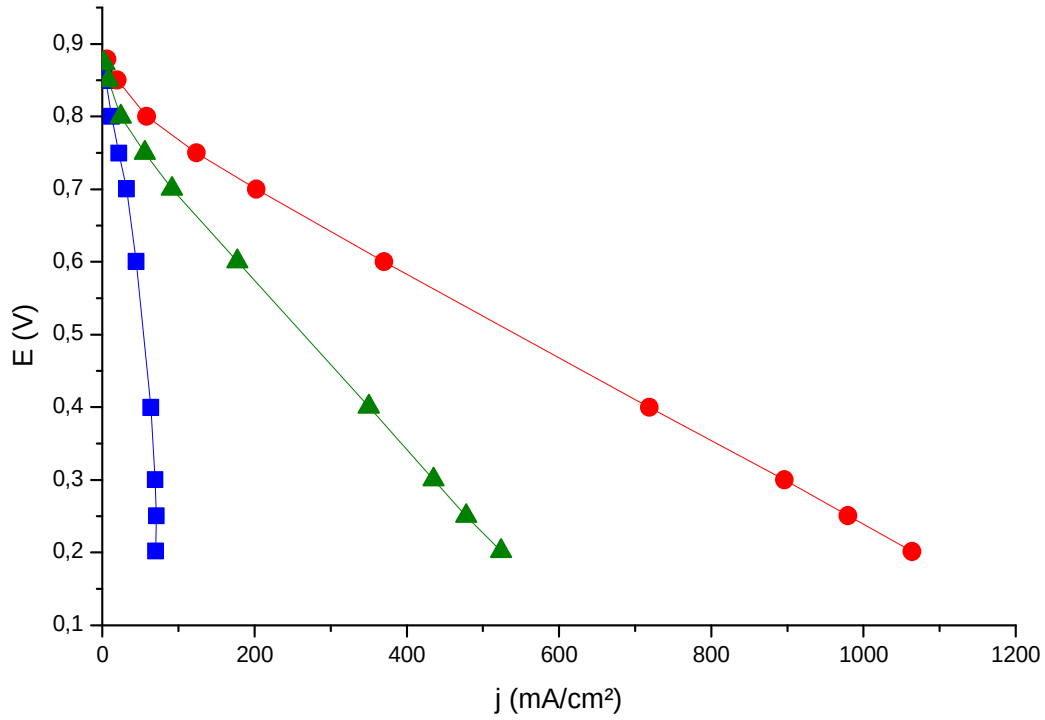


Figure 4. Cell voltage vs. experimental current density for A* (●), C* (■) and B* (▲).

Figure 5 represents the different contributions to losses for the three MEA. As expected from the MEA resistance values (Table 3), the ohmic losses (Figure 5b) are equivalent for A* and C*. As these MEA can only be differentiated by the aerogel used at the cathode and the two carbon aerogels have a very different texture, this result could mean that the carbon aerogel texture does not significantly affect the catalytic layer resistance.

So, the most interesting results are activation losses (Figure 5a) and diffusive losses (Figure 5c). Surprisingly, C* presents more important activation losses than A* whereas both MEA have almost the same active platinum surface area. Besides, Tafel slopes are not in the same range (Tafel slopes of C* is nearly twice as high as others Tafel slopes). Neyerlin at al. [15] showed (in PEMFC) that uncorrected $O_2$ mass-transport hindrance yields to higher (and poorly-defined) ORR Tafel slopes. This must be the case of C* as its pores are very small. Concerning A* and B*, the differences of activation losses must be due to a difference of active platinum surface area.

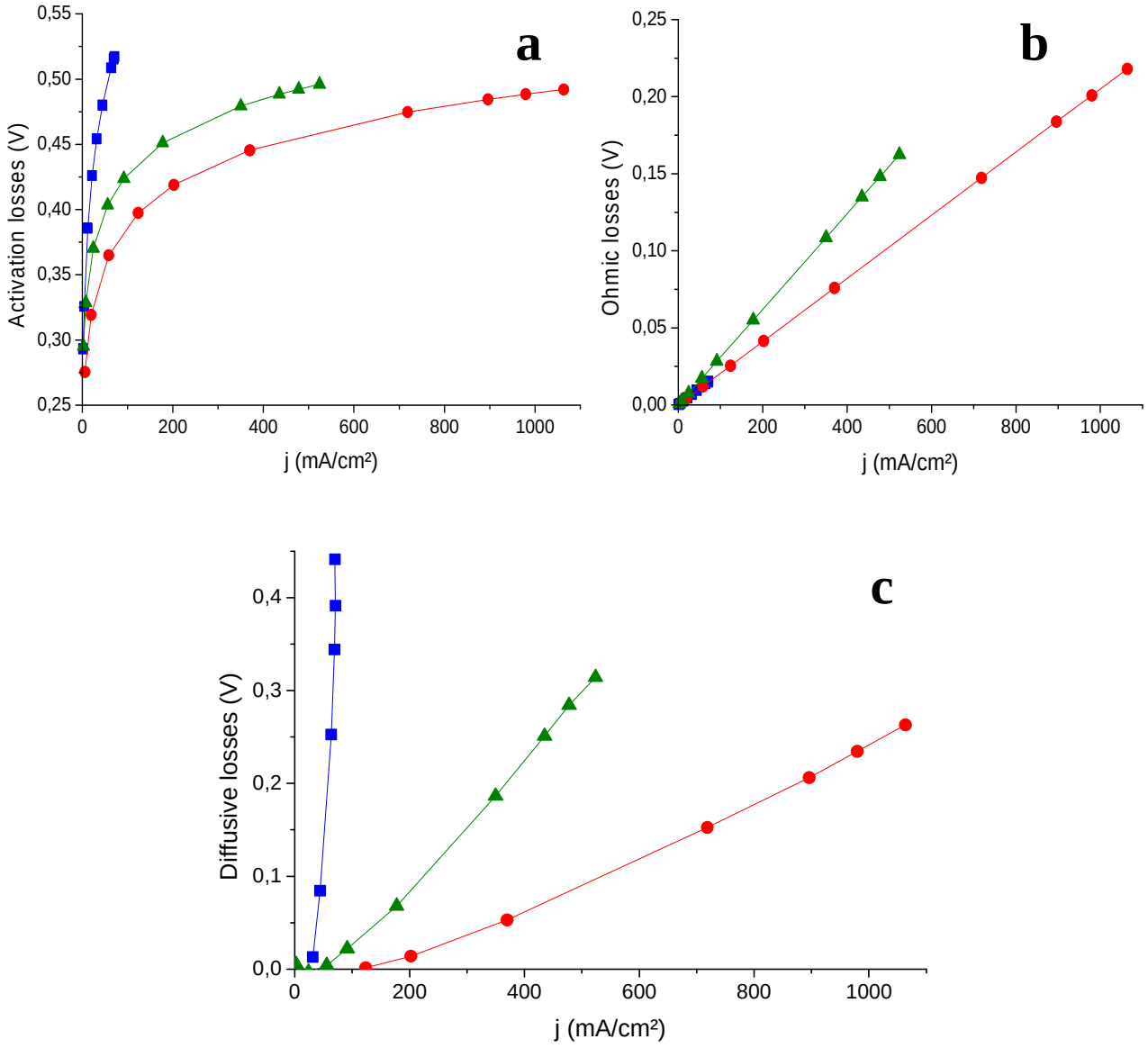


Figure 5. Activation losses (a), Ohmic losses (b) and diffusive losses (c) of A* (●),B* (▲) and C* (■).

Analyzing the diffusive losses (Figure 5c), we can conclude that the carbon aerogels texture greatly affects the performances. The smaller the pores, the higher the diffusive losses. That is the case for C*, the pores of which measure less than 30 nm (Hg porosimetry results); such small pore size hinders gas diffusion to the reaction sites. Small pores are indeed known to be detrimental in MEA as described by Uchida et al. [16], who showed that Nafion® could not penetrate in pores smaller than 40 nm. Moreover, small pores could slow down gases diffusion and are flooded more quickly, the latter phenomena also affecting gas diffusion. The differences between A* and B* can be explained by the smaller macroporous volume of B*. Comparing the synthesis parameters (%solid and R/C), we can conclude that the best results are obtained with the highest R/C ratio (R/C=200) and the lowest %solid (%solid=5). The R/C ratio affects the carbon

aerogel particles size: when R/C is low, the number of little particles increases; when R/C is high, the particles growth is facilitated [3]. The percentage of solid affects the aerogel density and mesopores size: when %solid diminishes, the aerogel density decreases and bigger mesopores are produced [1]. In summary, the performances of carbon aerogel supported nanoparticles seem to be enhanced for large aerogel particles containing large mesopores.

## 5. CONCLUSIONS

This study enabled us to highlight the impact of the catalytic layers architecture on the PEMFC performances. Carbon support texture plays an important role in the final performances of PEMFC. By varying the synthesis parameters of carbon aerogels we showed that these parameters affect their performances and that the carbon support texture must be controlled. Further investigations will be needed to determine the optimal synthesis parameters. We also demonstrated that Nafion® loading must be optimized when carbon aerogels are used. Investigations are in progress to confirm these results and to enlarge the panel of carbon aerogel morphologies and Nafion® loading in order to improve the understanding of the relations between architecture and performances.

## ACKNOWLEDGEMENTS

We thank N. Job (Université de Liège) for $N_2$ sorption and Hg porosimetry measurements. M.Y. Perrin (CEMEF, Ecole Nationale Supérieure des Mines de Paris) is also acknowledged for TEM analysis.

## REFERENCES

1. Fung A.W.P, 1995, Relationship between particle size and magnetoresistance in carbon aerogels prepared under different catalyst conditions, *J. Non-crystalline solids*, vol. 186: pp. 200-208.
2. Tamon H., Ishizaka H., Araki T., Okazaki M., 1998, Control of mesoporous structure of organic and carbon aerogels, *Carbon*, vol.36, issue 9: pp. 1257-1262.
3. Reynolds G.A.M., Fung A.W.P., Wang Z.H., Dresselhaus M.S., Pekala R.W., 1995, The effects of external conditions on the internal structure of carbon aerogels, *J. Non-crystalline solids*, vol. 188, issues 1-2: pp. 27-33.
4. Glora M., Wiener M., Petričević R., Pröbstle H., Fricke J., 2001, Integration of carbon aerogels in PEM fuel cells, *J. Non-crystalline solids*, vol. 285, issues 1-3: pp. 283-287.
5. Smirnova A., Dong X., Hara H., Vasiliev A., Sammes N., 2005, Novel carbon aerogel-supported catalysts for PEM fuel cell application, *Int J. Hydrogen energy*, vol. 30, issue 2: pp. 149-158.
6. Marie J., Chenitz R., Chatenet M., Berthon-Fabry S., Cornet N., Achard P., 2008, Highly porous PEMFC cathodes based on low density carbon aerogels as Pt-support : experimental study of the mass-transport losses, *Submitted to Journal of Power Sources*.
7. Marie J., Berthon-Fabry S., Achard P., Chatenet M., Chainet E., Pirard R., Cornet N., 2006, Synthesis of highly porous catalytic layers for Polymer Electrolyte Fuel Cell based on carbon aerogels, *ECS Transactions*, vol. 1, issue 6: pp. 509-519.
8. Pekala R.W., 1989, Organic aerogels from the polycondensation of resorcinol with formaldehyde, *Journal of Material Science*, vol. 24: pp. 3221-3227.
9. Marie J., Berthon-Fabry S., Achard P., Chatenet M., Pradourat A., Chainet E., 2004, Highly dispersed platinum on carbon aerogels as supported catalysts for PEM fuel cell-electrodes: comparison of two different synthesis paths, *J. Non-crystalline solids*, vol. 350: pp. 88-96.
10. Marie J., Berthon-Fabry S., Chatenet M., Chainet E., Pirard R., Cornet N., Achard P., 2007, Platinum supported on resorcinol-formaldehyde based carbon aerogels for PEMFC electrodes: Influence of the carbon support on electrocatalytic properties, *J. Applied Electrochemistry*, vol. 37, issue 1: pp. 147-153.
11. Marie J., 2007, Design, study and characterization of new PEM fuel cells electrode materials based on carbon aerogels. Processing them in membrane electrode assembly, *PhD thesis (Energetics), Ecole des Mines de Paris*. Confidential until 1/1/2009.

12. Gasteiger H.A., Kocha S.S., Sompalli B., Wagner F.T., 2005, Activity benchmarks and requirements for Pt, Pt-alloy, and non-Pt oxygen reduction catalysts for PEMFCs, *Applied Catalysis B: Environmental*, vol. 56, issues 1-2: pp. 9-35.
13. Passalacqua E., Lufrano F., Squadrito G., Patti A., Giorgi L., 2001, Nafion content in the catalyst layer of polymer electrolyte fuel cells: effects on structure and performance, *Electrochimica Acta*, vol. 46, issue 6: pp. 799-805.
14. Guilminot E., Corcella A., Chatenet M., Maillard F., 2007, Comparing the thin-film rotating disk electrode and the ultramicroelectrode with cavity techniques to study carbon-supported platinum for proton exchange membrane fuel cell applications, *J. Electroanalytical Chemistry*, vol. 599, issue 1: pp. 111-120.
15. Neyerlin K.C., Gu W., Jorne J., Clark A. Jr., Gasteiger H.A., 2007, Cathode catalyst utilization for the ORR in a PEMFC, Analytical model and experimental validation, *J. Electrochemical Society*, vol. 154, issue 2: pp. B279-B287.
16. Uchida M., Aoyama Y., Eda N., Ohta A., 1995, Investigation of the microstructure in the catalyst layer and effects of both perfluorosulfonate ionomer and PTFE-loaded carbon on the catalyst layer of polymer electrolyte fuel cells, *J. Electrochemical Society*, vol.142, issue 12: pp. 4143-4149.